HHS Public Access

Author manuscript

Nat Chem Biol. Author manuscript; available in PMC 2011 September 01.

Published in final edited form as:

Nat Chem Biol. 2011 March ; 7(3): 154–160. doi:10.1038/nchembio.512.

Radical-Mediated Enzymatic Carbon Chain Fragmentation-Recombination

Qi Zhang[1], **Yuxue Li**[2], **Dandan Chen**[1], **Yi Yu**[1], **Lian Duan**[1], **Ben Shen**[3], and **Wen Liu**[1,*]

[1]State Key Laboratory of Bioorganic and Natural Products Chemistry, Shanghai Institute of Organic Chemistry, Chinese Academy of Sciences, 345 Lingling Rd., Shanghai 200032, China

[2]State Key Laboratory of Organometallic Chemistry, Shanghai Institute of Organic Chemistry, Chinese Academy of Sciences, 345 Lingling Rd., Shanghai 200032, China

[3]Division of pharmaceutical Sciences, School of Pharmacy, University of Wisconsin-Madison, 777 Highland Ave., Madison, Wisconsin 53705, USA

Abstract

The radical *S*-adenosylmethionine (*S*-AdoMet) superfamily contains thousands of proteins that catalyze highly diverse conversions, most of which are poorly understood due to a lack of information regarding chemical products and radical-dependent transformations. We here report that NosL, involved in forming the indole side ring of the thiopeptide nosiheptide (NOS), is a radical *S*-AdoMet 3-methyl-2-indolic acid (MIA) synthase. NosL catalyzed an unprecedented carbon chain reconstitution of L-Trp to give MIA, showing removal of the Cα-N unit and shift of the carboxylate to the indole ring. Dissection of the enzymatic process upon the identification of products and a putative glycyl intermediate uncovered a radical-mediated, unusual fragmentation-recombination reaction. This finding unveiled a key step in radical *S*-AdoMet enzyme-catalyzed structural rearrangements during complex biotransformations. Additionally, NosL tolerated fluorinated L-Trps as the substrates, allowing for production of a regiospecifically halogenated thiopeptide that has not been found in over 80 entity-containing, naturally occurring thiopeptide family.

Thiopeptides are a class of clinically interesting and highly modified polythiazolyl antibiotics1–3. The potent activity of many members against various drug-resistant bacterial pathogens has promoted extensive investigations by chemical modification into new

*To whom correspondence should be addressed: Wen Liu, Shanghai Institute of Organic Chemistry, Chinese Academy of Sciences, 345 Lingling Rd., Shanghai 200032, China. wliu@mail.sioc.ac.cn, Tel: 86-21-54925111, Fax: 86-21-64166128.

Author contributions

Q.Z., D.C., Y.Y. and L.D. provided the experimental evidences; Y.L. performed the theoretical calculations; Q.Z., B.S. and W.L. analyzed the data and wrote the paper; and W.L. designed the research. All authors discussed results and approved the final manuscript.

Competing financial interests

The authors declare no competing financial interests.

Additional information

Supplementary information is available online at http://xxxx

analogue development, towards overcoming their physical drawbacks such as water solubility for clinical use. Thiopeptides possess a characteristic macrocyclic core, consisting of a nitrogen-containing, 6-membered ring central to multiple thiazoles and dehydroamino acids, but vary in side chain (and/or ring) appending additional functionalities (Fig. 1a). In contrast to heroic efforts of chemical synthesis4, their newly established biosynthetic pathways for thiopeptide framework formation are remarkably concise5–11, showing conserved posttranslational modifications on a ribosomally synthesized precursor peptide. The reactions include cyclodehydrations and subsequent dehydrogenations to form aromatic thiazoles, dehydrations to generate dehydroamino acids, and an intramolecular cyclization to afford the nitrogen heterocycle.

For most polycyclic thiopeptides, the side ring formations are precursor peptide-independent12–16. They exclusively exploit L-Trp to furnish the variable functional groups, as exemplified by the indolic acid moiety of nosiheptide (NOS) and the quinalic acid moiety of thiostrepton (Fig. 1b). Whereas the quinalic acid formation may require seven enzymes to convert L-Trp in a process including methylation, desamination, oxidation, ring opening and recyclization, reduction, and epoxidation6,7, the indolic acid moiety formation in NOS biosynthesis involves two enzymes NosL and NosN, both of which encodes the putative radical *S*-adenosylmethionine (*S*-AdoMet) proteins, to process L-Trp via a completely different route9. Characterization of a side ring opened NOS analogue by inactivating *nosN* supported the methylation activity of NosN, which acts on the 3-methylindolyl group to furnish the 3,4-dimehtylindole moiety. This leaves NosL as a candidate to biosynthesize the key intermediate, 3-methyl-2-indolic acid (MIA, **1**). We have confirmed the essentiality of NosL to MIA formation9,11: inactivation of *nosL* completely abolished NOS production, which can be restored either by feeding extraneous **1** or by heterologous complementation with its counterpart *nocL* from nocathiacin (a naturally occurring analogue of NOS) biosynthesis. However, whether NosL alone catalyzes such a complex conversion remains elusive, given that **1** biosynthesis from L-Trp requires multiple, chemically unusual reactions to process the carbon side chain (including removal of the Cα-N unit and shift of the carboxylate to the indole ring. Fig. 1b).

In this study, we characterized NosL indeed as a radical *S*-AdoMet protein for converting L-Trp to MIA, the process of which involves a radical-mediated, unusual fragmentation-recombination reaction. This characterization took advantage of efficient **1** production in the *nosL*-expressing *Escherichia coli* strain and *in vivo* and/or *in vitro* determination of substrate(s), products (including shunt products), and a putative glycyl intermediate in NosL-catalyzed conversion. In light of the substrate tolerance of NosL, regiospecific fluorination of NOS was achieved via a modified MIA intermediate, yielding a new halogenated thiopeptide that has not been found in the naturally occurring family.

RESULTS

In vivo validation of NosL as a MIA synthase

Considering that radical *S*-AdoMet proteins are sensitive to O_2 for *in vitro* study in general17, we first set out to investigate the NosL function *in vivo*. *nosL* was introduced to and expressed in *E. coli* BL21(DE3), yielding the recombinant strain SL4101 to produce

NosL in a *N*-terminally 6 × His-Tagged form. High performance liquid chromatography (HPLC) analysis revealed a compound produced by SL4101, which was absent in the control strain SL4100 carrying the vector alone (Fig. 2a). The molecular formula $C_{10}H_9O_2N$ for this compound was established by high-resolution (HR)-electron spray ionization (ESI)-Mass spectroscopy (MS), showing a $[M - H]^-$ ion at *m/z* = 174.05605 (174.05615 calculated). Additionally, ^1H, ^{13}C and selected 2D NMR analyses confirmed it to be **1**, indicating that NosL is a novel MIA synthase. To probe the origin of **1**, the *nosL*-expressing cells of SL4101 from Luria-Bertani (LB) broth were harvested, and inoculated into a nutrient-insufficient medium followed by further incubation with individual amino acids for a time course analysis of **1** production. Only the addition of L-Trp sped up **1** formation with the apparent rate of 150 μg/L per min in the initial 4 h, whereas the supplementation of other amino acid such as L-Gly or L-Ser had no significant effect on the **1**-producing rate (Supplementary Fig. 1). This validated that L-Trp serves as the substrate for the production of **1**. The relatively high yield of **1** (42 ± 5 mg/L over a 20-hour period) facilitated its purification and enabled further *in vivo* experiments to examine NosL catalysis.

NosL as a Radical *S*-AdoMet protein for MIA formation

Based on sequence alignment NosL falls into the ThiH radical *S*-AdoMet subclass (around 20% identity, Supplementary Fig. 2), possessing a typical CxxxCxxC motif for [4Fe-4S] cluster nucleation and a Gly-containing segment involved in *S*-AdoMet binding. We therefore explored the nature of NosL for its cofactor binding and subsequent chemical transformations. In the CxxxCxxC motif, the Cys residues (corresponding to C95, C99 and C102) were systematically replaced to Ala. The constructs were introduced into *E. coli* BL21(DE3), yielding the recombinant strains SL4103 (for AxxxCxxC mutation of NosL), SL4105 (for CxxxAxxC mutation), and SL4107 (for CxxxCxxA mutation) for MIA (**1**) examination. These replacements completely abolished **1** production (Supplementary Fig. 3), demonstrating their indispensability to the NosL activity. The *S*-AdoMet binding potential was also evaluated in a similar way, by replacing G142 to Ala within the conserved GE/D motif. The recombinant strain SL4109 for expressing mutant NosL (G142A) lost the ability to produce **1** (Supplementary Fig. 3), supporting that NosL is a *S*-AdoMet-dependent protein.

Next, NosL was purified from SL4101 to homogeneity for assays *in vitro*. Whereas the aerobically isolated enzyme was inactive, the activity of the anaerobically isolated NosL was detectable but extremely low (Supplementary Fig. 4). NosL was then reconstituted under a strictly anaerobic condition, giving the purified sample (Supplementary Fig. 5a) in dark brownish color. This protein contained 5.1 ± 0.5 of Fe and 5.7 ± 0.3 of sulfide per molecule. The ultraviolet (UV)-visible absorptions of the reconstituted NosL are characteristic for [4Fe-4S] binding proteins (Supplementary Fig. 5b), displaying a A280/A400 ratio at 3.4 : 1 and an apparent shift by reducing with sodium dithionite. Further electron paramagnetic resonance (EPR) analysis at 13 K gave an axial spectrum (Supplementary Fig. 5c), showing approximate *g* values of 2.02 and 1.91. This supported the binding of a $[4Fe\text{-}4S]^+$ cluster to NosL. Incubation of the reconstituted NosL with L-Trp and *S*-AdoMet was performed in the presence of dithionite, indeed showing MIA (**1**) production with the yield approximately 7-fold higher than that of the as-isolated enzyme without reconstitution (Fig. 2a and

Supplementary Fig. 4a). In the reaction mixture the chemical reductant dithionite can be replaced with a natural reduction system containing flavodoxin, flavodoxin reductase, and NADPH, leading to ~100% improvement in **1** formation (Supplementary Fig. 6). NosL-catalyzed conversion cannot proceed in the absence of *S*-AdoMet (Fig. 2a), turn-over of which by NosL was further confirmed upon identification of the product 5'-deoxyadenosine (AdoH, **2**, Fig. 2b). *S*-AdoMet consumption was independent of L-Trp, but significantly enhanced by adding L-Trp into the reaction mixture (Fig. 2b and Supplementary Fig. 4a). Together with the identification of methionine (discussed below) as the concomitant product originating from *S*-AdoMet, we conclude that NosL, whose activity is *S*-AdoMet-dependent, catalyzes **1** formation from L-Trp via an Ado$^{\bullet}$-initiated process.

NosL-catalyzed carbon chain reconstitution on L-Trp

To investigate the mechanism of NosL-catalyzed conversion, we focused on the reconstitution of the carbon side chain of L-Trp. [1-^{13}C] and [3-^{13}C]-labeled L-Trps were fed individually into SL4101, resulting in enriched ^{13}C resonances for the 2-carboxylate (at δ 164.0 for product **3**) and 3-methyl group (at δ 8.83 for product **4**) of MIA, respectively (Scheme 1 and Supplementary Fig. 7). Consistent with similar studies carried out in the NOS-producing strain *Streptomyces actuosus*12,13, these findings demonstrated that **1** biosynthesis involves an unprecedented carbon chain rearrangement of the L-Trp precursor, showing 1) the intramolecular migration of the carboxylate to C2 of the indole ring, 2) transformation of the methylene carbon to a methyl group, and 3) elimination of the α-carbon and its associated amino group. The feeding of L-[$^{2}H_8$]-Trp also supported this conclusion by allowing the production of [$^{2}H_6$]-MIA (**5**) (HR-ESI-MS *m/z* calcd. for $C_{10}D_6H_2O_2N$ 180.09371, found 180.09343), and excluded the participation of the benzene ring in this conversion (given no change in deuterium substitutions, Scheme 1). A 0.04 ppm upfield-shift (from δ 2.48 relative to CH_3) of the signal that corresponds to the CHD_2 protons was found in the ^{1}H NMR spectrum of **5** (Supplementary Fig. 8), ruling out adjacent hydrogen transfer, either from Cα or from C2 on the indole ring, to provide the third hydrogen atom of the methyl group. Further, using L-[$^{2}H_8$]-Trp as the substrate, *in vitro* assay of NosL-catalyzed reactions showed that the co-produced AdoH (**2**) (HR-ESI-MS *m/z* calcd. for $C_{10}H_{13}N_5O_3$ 252.10967, found 252.10983) was not deuterium labeled. This clearly indicates that the Ado$^{\bullet}$-initiated rearrangement of the carbon chain does not start with a C-H bond cleavage on L-Trp to generate the substrate radical.

Determination of the coproduct and shunt products

To probe the individual steps in MIA (**1**) formation, we carried out extensive survey of the product profile in NosL-catalyzed *in vitro* conversion. HPLC analysis of the reaction mixture revealed the first shunt product (Fig. 2a), which was deduced to be 3-methylindole (**6**) upon further GC-MS analysis with an authentic compound as the standard (Supplementary Fig. 9). Supplementation with 2,4-dinitrophenyl hydrazine (DNP) for derivatization led to identification of the second shunt product as glyoxylate (**7**) (corresponding to **8**, the derivative 2-(2,4-dinitrophenyl) hydrazonoacetate. Fig. 2c and Supplementary Fig. 10). Thus, the first Cα-Cβ cleavage of L-Trp appears to provide the 3-methylindole part whereas the readdition-coupled, second cleavage may take place on the

separated 2C-N unit to furnish the 2-carboxylate group. Consistent with this prediction, upon a similar derivatization we detected the production of formaldehyde (**9**) (corresponding to **10**, the derivative 1-(2,4-dinitrophenyl)-2-methylene hydrazine. Fig. 2c and Supplementary Fig. 11), which most likely comes from the α-carbon of L-Trp.

Quantitative analysis of NosL-catalyzed *in vitro* reaction

We chose three representative products, including MIA (**1**) and 3-methylindole (**6**) from L-Trp, and AdoH (**2**) from *S*-AdoMet, to quantitatively evaluate NosL-catalyzed *in vitro* conversion (Supplementary Fig. 4). The yields of the products were enzyme dose-dependent, as the increase of the concentration of NosL accordingly improved the production of **1, 6**, and **2** (Supplementary Fig. 4a). Their productions at 25°C were relatively constant in the presence of 1 mM dithionite, 500 μM L-Trp and 1 mM *S*-AdoMet, showing that about 39 ± 3 μM **1**, 140 ± 20 μM **6** and 381 ± 30 μM **2**, with a ratio around 1 : 3.6 : 9.8, were produced by 20 μM NosL catalysis over a two-hour period (Supplementary Fig. 4b). For conversion of the substrate L-Trp, under this condition one molecule of NosL produced approximate two molecules of **1** along with seven molecules of **6**. The production of AdoH was consistently higher, showing a yield ratio around 2.1 : 1 for **2** corresponding to a sum of **1** and **6**. For optimizing the reaction, we speculated that the reduction degree in the reaction mixture may impact the proportion of **1**. We therefore measured the effect of the concentration of the chemical reductant dithionite on the yields of **1** and **6** (Supplementary Fig. 4c). Intriguingly, **6** production was highly dependent of dithionite concentration, whereas the yields of **1** were relative constant, around 30–42 μM in all assays. Particularly, when 100 μM dithionite was used, the ratio of **1** to **6** can be improved to around 3 : 1.

Prediction of the Cα-Cβ bond cleavage manner on L-Trp

Inspired by identification of 3-methylindole (**6**) and glyoxylate (**7**) as the shunt products, we proposed that the Ado$^{\bullet}$-initiated carbon chain reconstitution of L-Trp may begin with a Cα-Cβ bond cleavage during NosL-catalyzed MIA (**1**) formation. According to the bond-breaking pattern, either via homolysis or via heterolysis, there are two sets of hypothetic intermediates that share a common fate to the shunt product pair (Fig. 3). Thus, the Density Functional Theory (DFT) calculation was performed to differentiate these two possibilities (Fig. 3, and Supplementary Figs. 12 and 13). While the direct cleavage of the L-Trp neutral radical (**11**) as outlined in **Path 1** leads to the generation of the intermediates **12** and **13** (heterolytic) or **14** and **15** (homolytic), **Path 2** indicates that the cleavage accompanied with an intramolecular hydrogen migration results in the production of the intermediates **16** and **17** (heterolytic) or **18** and **19** (homolytic). Given the intermediate **11** that may get a proton from the environment, the model shown in **Path 3** is also considered, indicating the generation of the intermediates **16** and **20** (heterolytic) or **18** and **15** (homolytic). At all events the homolytic products are lower in energy than their corresponding heterolytic products, suggesting that the homolysis was thermodynamically favored to form 3-metheneindole and glycyl radical.

To experimentally support the hypothesis, we attempted to probe the putative intermediate in NosL-catalyzed reaction, by employing a derivatization associated, rapid quench method previously used for analyzing the glutamate mutase-catalyzed reaction. Glutamate mutase, a

Ado•-producing, adenosylcobalamin (AdoCbl, coenzyme B_{12})-dependent protein, has been demonstrated to convert L-Glu into glycyl radical (trapped as glycine by using this quench technique) and acrylate during L-*threo*-3-methylaspartate formation18–20. The NosL-catalyzed reaction was quenched at 10 sec before derivatization with dansyl chloride. HPLC-MS analysis showed the production of glycine (**21**) (corresponding to the derivative Gly-dansyl, **22**. Fig. 2d and Supplementary Fig. 14), as well as methionine (**23**) (corresponding to the derivative Met-dansyl, **24**. Fig. 2d and Supplementary Fig. 15) deriving from *S*-AdoMet. Using Asn as an internal standard, the glycine species was observed in a yield of 2 ± 0.5 μM, equal to around 2.5% of the enzyme active site. Under the highly reductive condition this species is presumed to derive from the immediately uncoupled intermediate, glycyl radical, consistent with the predicted manner for homolytic cleavage of the Cα-Cβ bond of L-Trp during MIA formation.

Substrate flexibility of NosL

Unveiling of the NosL chemistry then promoted us to feed available analogues of L-Trp, including D-Trp and derivatives with different substitutions on the indole ring, into SL4101 to determine the substrate tolerance of NosL. Individual additions of most of these substrates had no effect on MIA (**1**) production, and failed to afford the expected **1** analogues (Supplementary Table 3). These indicate the stringent substrate specificity of NosL in stereochemistry and in functionalization of the indole ring. In contrast, feeding of 5- or 6-fluoro-DL-Trp (only the L-configuration isomer can be used as the substrate) led to generation of the distinct product with a yield approximately 20% of the concomitant **1** production (Supplementary Fig. 16). Spectroscopic analyses, including HR-ESI-MS, and ^{1}H, ^{13}C and ^{19}F NMR (Supplementary Fig. 17), clearly established these compounds corresponding to 5-fluoro-MIA (**25**) and 6-fluoro-MIA (**26**), respectively (Scheme 1).

Generation of a fluorinated NOS analogue

To determine whether or not the fluorinated MIA (**1**) can be incorporated as an intermediate *in vivo*, we therefore fed 5-fluoro-DL-Trp into the NOS-producing strain *S. actuosus*. HPLC-MS analysis showed the dramatic decrease in NOS production (20%–25% relative to that of the wild type strain, Fig. 4), presumably due to competitive inhibition of biosynthetic enzymes in the substrates. A new product, with UV spectra similar to NOS, was clearly observed, showing a yield approximately 20% of the concomitant NOS production. According to the molecular formula as $C_{51}H_{42}FN_{13}O_{12}$ (HR-ESI-MS *m/z* calcd. 1238.13114, found 1238.12959), this compound was deduced to be a NOS analogue substituted by a fluorine atom at C5’ of the indole ring (Fig. 1a and Supplementary Fig. 18). For structural elucidation it was purified and then subjected to comparative spectroscopic analysis with NOS, showing the only difference in the indole moiety. ^{19}F NMR, and 1D and 2D NMR spectra further supported this structure assignment of 5’-fluoro-NOS (**27**. Supplementary Fig. 19 and Table 4). The effect of the 5’-fluoro-substitution on antibacterial activity was consequently evaluated by bioassays against the test strain *Bacillus subtillis*, displaying the minimum inhibitory concentration (MIC) at 0.004 μM/mL for **27** to that at 0.008 μM/mL for NOS (Supplementary Table 5), Notably, there has yet to be a halogenated

member of the naturally occurring thiopeptide antibiotics, which number over 80 compounds reported to date1.

DISCUSSION

The radical *S*-AdoMet superfamily currently comprises thousands of proteins that participate in numerous biochemical processes in animals, plants, and microorganisms17,21–24. These proteins share a common mechanism to generate a powerful oxidant Ado$^{\bullet}$, thereby initiating highly diverse transformations relevant to DNA repair and in the biosynthesis of vitamins, coenzymes, and antibiotics. Biochemical mechanisms of most of such conversions have not been characterized, due to a lack of information about the enzyme functions and radical-mediated transformations. Focusing on the characterization of NosL and NosL-catalyzed reaction, we herein unveiled a radical-mediated, unusual fragmentation-recombination process, which represents a key step in understanding radical *S*-AdoMet enzyme-catalyzed complex structure rearrangements.

The mechanism for NosL-catalyzed reaction was proposed in Scheme 2. Distinct from the widely found, C-H bond cleavage in the reactions controlled by known radical *S*-AdoMet enzymes17, Ado$^{\bullet}$ in NosL catalysis may abstract the hydrogen atom from N_1 on the indole ring of L-Trp to generate **11**, the neutral substrate radical. The homolysis is thermodynamically favorable, leading to the Cα-Cβ bond cleavage for the first fragmentation to give the transient units 3-metheneindole and glycine radical. Taking a simultaneous proton transfer into account, the resulting cationic 3-metheneindole (**18**) and glycine radical (**19**) are more stable, facilitating their subsequent re-addition to generate the radical intermediate **28** (**Mechanism 1**). Elimination of the Cα-N unit (giving the methanimine radical **29**) from **28** can proceed to furnish the 2-carboxylate group to yield MIA (**1**), and the hydrogen rebound to **29** results in the production of CH_2=NH, which is hydrolyzed in the aqueous medium to form formaldehyde (**9**) and ammonia. Alternatively, according to a glycine decarboxylation-based free radical mechanism proposed previously25, the second fragmentation on the separated 2C-N unit (glycyl radical **15**) could precede the re-addition, and results in a direct reposition of the carboxylate at C-2 of the indole ring (**Mechanism 2**): 1) the protonated radical **15** may undergo a C-C bond cleavage to generate carboxyl radical **30**; and 2) the addition of **30** to 3-mtheneindole **14** can yield radical **31**, hydrogen rebound to which eventually leads to the production of **1**.

NosL-catalyzed *in vitro* conversion produced **1** along with two shunt products 3-methylindole (**6**) and glyoxylate (**7**), which may originate from the intermediate pair 3-metheneindole and glycyl radical, respectively. We proposed that the Cα-Cβ bond cleavage-post biotransformation, such as the inefficient recombination, may serve as a limitation step in NosL-catalyzed *in vitro* process. The over-produced intermediates could be released from the active site of NosL into the aqueous medium: while 3-metheneindole is aromatized by reduction to **6**, glycyl radical is rapidly degraded to **7** and ammonia. The one electron-unpaired organic radicals have been known to be highly active and unstable. For instance the substrate-based, proposed glycyl radical (Scheme 2), if it fails to be further processed (e.g. addition to the intermediate 3-metheneindole), may lose an electron to generate dehydroglycine followed by hydrolysis for glyoxylate production. The similar result has

been found in the *in vitro* reaction catalyzed by ThiH26. Without the associated components for turning over gylcyl radical or dehydroglycine in thiazole formation, ThiH catalyzes the Cα-Cβ bond cleavage of L-Tyr and gives *p*-cresol and glyoxylate as the products.

Substrate fragmentation is known in Ado•-induced biotransformations, as exemplified by ThiH and by newly characterized HydG (24% identity to NosL)27, which catalyzes the L-Tyr cleavage to generate *p*-cresol and cyanide. NosL, ThiH and HydG may share a common paradigm to process the radical-based, aromatic amino acid substrates for the Cα-Cβ bond cleavage, despite their difference in the fate of the resulting gylcyl radical (or dehydroglycine) intermediate. However, the fragmentation-recombination found in NosL chemistry is rare. To our knowledge, the only known example is glutamate mutase, the radical AdoCbl-dependent protein that converts L-Glu to the β-methyl branched product (but without fragment elimination)20,24. This strategy might be employed in certain Ado•-mediated structural rearrangements, such as the ThiC-catalyzed complex conversion of 5-aminoimidazole ribonucleotide to 4-amino-5-hydroxymethyl-2-methylpyrimidine phosphate in thiamine biosynthesis28.

In conclusion, we have uncovered NosL as a MIA synthase that catalyzes an unprecedented carbon side chain reconstitution of L-Trp. The radical-mediated, unusual fragmentation-recombination process may be general for radical *S*-AdoMet protein-catalyzed structural rearrangements in certain uncharacterized biotransformations. Taking advantage of the substrate tolerance of NosL, regiospecific fluorination of NOS could be achieved via a modified MIA intermediate. The NOS analogue produced in this fashion and bearing fluorine at the 5' position showed the improved pharmaceutical property. This application of combinatorial biosynthesis, enabled by our elucidation of NosL chemistry, compliments recent advances in understanding sequence permutations of the precursor peptide29,30.

METHODS

Bacterial strains, plasmids and primers

Please see Supplementary Tables 1 and 2

Materials

Please see Supplementary Methods.

Production of MIA *in vivo*

Construction of the recombinant strain SL4101 for expressing *nosL* was described in Supplementary Methods. SL4101 was cultured in LB medium. Once the cell density reached 0.6–0.8 at $OD_{600\ nm}$, the $Fe(NH_4)_2SO_4$ solution was added into the culture broth to a concentration of 50 μM, followed by incubation on ice for 10 min. After addition of isopropyl-β-D-thiogalactopyranoside (IPTG, 100 μM in final), *nosL* expression had been induced at 25°C for 6–8 h. While the cells were harvested by centrifugation for following experiments (see below), the supernatant was directly subjected to HPLC analysisfor product examination. SL4100 carrring the vector pET28a alone was utilized as the control in

the parallel analytic process. Site-specific mutagenesis for exploring the cofactor binding nature of NosL was described in Supplementary Methods.

Time Course-Based Analysis of MIA Production *in vivo*

The harvested SL4101 cells described above were resuspended in a nutrient-insufficient medium (yeast extract 0.1%, tryptone 0.5%, glucose 0.4%, NaCl 0.5%, glutamine 0.05%, K_2HPO_4 0.2%, $MgSO_4$ 0.01%, and $FeSO_4$ 0.001%), with $OD_{600\ nm}$ of 0.6–0.8. Variable amino acids, including L-Trp, L-Ser and L-Gly, were individually supplemented to the broth (5 mM in final) before further incubation at 28°C. MIA production was measured by HPLC at 0.5, 1, 2, 3, 4, 10, or 20 h. The MIA production is approximately linear with respect to time in initial 4 hr, and the apparent rate was accordingly estimated.

Feeding of Isotope Labeled L-Trps and Variable L-Trp Analogues

The procedure is similar to that of the time course-based analysis for MIA production, except the individual supplementation of isotope labeled substrates (i.e. L-[$^2H_8$]-Trp, L-[1-^{13}C]-Trp and L-[3-^{13}C]-Trp), D-Trp, and derivatives with different substitution on the indole ring (i.e. 1-methyl-L-Trp, 2-methyl-DL-Trp, 4-methyl-DL-Trp, 6-methyl-DL-Trp, 5-hydroxyl-L-Trp, 5-methoxy-DL-Trp, 5-bromo-DL-Trp, 5-fluoro-DL-Trp, and 6-fluoro-DL-Trp) to a concentration of 1 mM before further incubation at 28°C for 8 h. The production of labeled or functionally substituted MIAs was monitored by HPLC-MS.

Structural characterization of MIA and its analogues, and a new NOS analogue by feeding 5-fluoro-DL-Trp into the NOS-producing strain was summarized in Supplementary Methods.

Reconstitution of NosL

Production and anaerobic purification of NosL were summarized in Supplementary Methods. A previously reported procedure31 was modified to reconstitute the active enzyme. Dithiothreitol was added to the purified protein (10 mM in final). Under this reductive condition, $Fe(NH_4)_2SO_4$ solution (50 mM) was added carefully into the suspension to a final concentration of 500 μM. After 10 min, Na_2S solution (50 mM) was added in the same way to a concentration of 500 μM. The solution had been incubated on ice for 5–7 h. The resulting dark brown suspension was then subjected to desalting on a column (10-DG, Bio-Rad, USA) that was pre-equilibrated with the elution buffer (50 mM Tris-HCl, 25 mM NaCl, 10 mM dithiothreitol, and 10% glycerol, pH 8.0). The colored fraction was collected, and concentrated to 100 μM for *in vitro* assay. Protein characterization was described in Supplementary Methods.

Assay of the NosL activity *in vitro*

The 100 μL of reaction mixture contained 10 mM dithiothreitol, 500 μM dithionite, 200 μM *S*-AdoMet, 200 μM L-Trp (or L-[$^2H_8$]Trp), and 20 μM reconstituted NosL in 50 mM Tris-HCl buffer (pH 8.0). Reactions were initiated by adding of *S*-AdoMet to the 10 min pre-incubated mixture (as a negative control that contains the components except *S*-AdoMet), and then incubated at 25°C for 2 h. To terminate the reaction, trifluoroacetic acid (TFA) was added to a final concentration of 10% (v/v) to inactivate the enzyme. After removal of the

precipitates by centrifugation, the supernatant was subjected to HPLC-MS analysis. For evaluation of a natural reduction system, the chemical reductant dithionite was replaced by 0.5 mM NADPH, 50 μM flavodoxin, 20 μM flavodoxin reductase.

For GC-MS analysis, the supernatant was further extracted by ethyl acetate. For derivatization, 2,4-dinitrophenylhydrazine (DNP) was added to the supernatant (10 mM in final), which was further incubated at 37°C for 30 min.

Quantitative analysis of product formation *in vitro*

The 100 μL of reaction mixture contained 10 mM dithiothreitol, 1 mM dithionite, 1 mM *S*-AdoMet, and 500 μM L-Trp, in 50 mM Tris-HCl buffer (pH 8.0). The reconstituted NosL varying in concentration (10 μM, 20 μM, 40 μM, or 80 μM) was added into each reaction mixture. The 20 μM NosL catalysis was used for a time course analysis (by terminating at 10 min, 30 min, 60 min, 90 min, or 120 min). To measure the effect of dithionite concentration on the yields of MIA and 3-methylindole, each 100 μM of reaction mixture contained 20 μM reconstituted NosL, 10 mM dithiothreitol, 1 mM SAM, 500 μM L-Trp, and dithionite varying in concentration (100 μM, 200 μM, 500 μM, 1 mM, 2 mM, or 4 mM) in 50 mM Tris-HCl buffer (pH 8.0). The workups for the initiation, incubation and termination of reactions, and for the analysis of products were identical to those described above.

Probing of the putative intermediate in NosL-Catalyzed Conversion

Trapping of glycine species in NosL-catalyzed conversion was performed according to a modified procedure18. The 100 μL of reaction mixture contained 20 mM dithiothreitol, 2 mM dithionite, 1 mM *S*-AdoMet, 1 mM L-Trp, and 80 μM reduced NosL in 50 mM Tris-HCl buffer (pH 8.0). Reactions were initiated by adding of *S*-AdoMet to the 10 min pre-incubated mixture (as a negative control that contains the components except *S*-AdoMet) followed by immediately mixing, and then terminated at 10 sec by addition of TFA to a final concentration of 15% (v/v) to precipitate the enzyme. After removal of the precipitate by centrifugation, Na_2CO_3 (1.5 M in final) and dansyl chloride (1 mM in final) were supplemented to the supernatant, which was further incubated at 50°C for 60 min. 20 μL of TFA was then added to the solution, and the dansyl derivatives were subjected to HPLC-MS analysis. For quantifying the yield of glycine species, the amino acid Asn (20 μM) was used as an internal standard.

Supplementary Material

Refer to Web version on PubMed Central for supplementary material.

Acknowledgements

We thank Prof. H. G. Floss, University of Washington, for providing of *S. actuosus* ATCC25421 and his pioneer work on NOS biosynthesis, and Prof. Yuheng Zhang and Dr. Wei Tong, High Magnetic Field Laboratory, Chinese Academy of Sciences, for the assistance of EPR analysis. This work was supported in part by grants from National Institutes of Health of U.S (CA094426 to B.S.), National Natural Science Foundation (20832009, 30525001 and 20921091), Ministry of Science and Technology (2009ZX09501-008), National Basic Research Program (“973 program”, 2010CB833200), Chinese Academy of Sciences (KJCX2-YW-H08 and KSCX2-YW-G-06), and Science and Technology Commission of Shanghai Municipality (09QH1402700) of China (all to W.L).

References

1. Bagley MC, Dale JW, Merritt EA, Xiong X. Thiopeptide antibiotics. Chem. Rev. 2005; 105:685–714. [PubMed: 15700961]
2. Arndt H-D, Schoof S, Lu J-Y. Thiopeptide antibiotic biosynthesis. Angew. Chem. Int. Ed. 2009; 48:6770–6773.
3. Li C, Kelly WL. Recent advances in thiopeptide antibiotic biosynthesis. Nat. Prod. Rep. 2010; 27:153–164. [PubMed: 20111801]
4. Nicolaou KC, Chen JS, Edmonds DJ, Estrada AA. Recent advances in the chemistry and biology of naturally occurring antibiotics. Angew. Chem. Int. Ed. 2009; 48:660–719.
5. Brown LCW, Acker MG, Clardy J, Walsh CT, Fischbach MA. Thirteen posttranslational modifications convert a 14-residue peptide into the antibiotic thiocillin. Proc. Natl. Acad. Sci. USA. 2009; 106:2549–2553. [PubMed: 19196969]
6. Liao R, et al. Thiopeptide biosynthesis featuring ribosomally synthesized precursor peptides and conserved posttranslational modifications. Chem. Biol. 2009; 16:141–147. [PubMed: 19246004]
7. Kelly WL, Pan L, Li C. Thiostrepton biosynthesis: prototype for a new family of bacteriocins. J. Am. Chem. Soc. 2009; 131:4327–4334. [PubMed: 19265401]
8. Morris RP, et al. Ribosomally synthesized thiopeptide antibiotics targeting elongation factor Tu. J. Am. Chem. Soc. 2009; 131:5946–4955. [PubMed: 19338336]
9. Yu Y, et al. Nosiheptide biosynthesis featuring a unique indole side ring formation on the characteristic thiopeptide framework. ACS Chem. Biol. 2009; 4:855–864. [PubMed: 19678698]
10. Wang J, et al. Identification and analysis of the biosynthetic gene cluster encoding the thiopeptide antibiotic cyclothiazomycin in *Streptomyces hygroscopicus* 10–22. Appl. Environ. Microbiol. 2010; 76:2335–2344. [PubMed: 20154110]
11. Ding Y, et al. Moving posttranslational modifications forward to biosynthesize the glycosylated thiopeptide nocathiacin I in *Nocardia sp*. ATCC202099. Mol. BioSyst. 2010; 6:1180–1185.
12. Houck DR, Chen L-C, Keller PJ, Beale JM, Floss HG. Biosynthesis of the modified peptide antibiotic nosiheptide in *Streptomyces actuosus*. J. Am. Chem. Soc. 1988; 110:5800–5806.
13. Mocek U, et al. Biosynthesis of the modified peptide antibiotic nosiheptide in *Streptomyces actuosus*. J. Am. Chem. Soc. 1993; 115:7557–7568.
14. Mocek U, et al. Biosynthesis of the modified peptide antibiotic thiostrepton in *Streptomyces azureus* and *Streptomyces laurentii*. J. Am. Chem. Soc. 1993; 115:7992–8001.
15. Smith TM, Priestley ND, Knaggs AR, Nguyen T, Floss HG. 3,4-Dimethylindole-2-carboxylate and 4-(1-Hydroxyethyl)-2-quinolinecarboxylate activating enzymes from the nosiheptide and thiostrepton producers, *Streptomyces actuosus* and *Streptomyces laurentii*. J. Chem. Soc. Chem. Commun. 1993; 21:1612–1614.
16. Priestley ND, et al. Studies on the biosynthesis of thiostrepton: 4-(1-hydroxyethyl)-quinoline-2-carboxylate as a free intermediate on the pathway to the quinaldic acid moiety. Bioorg. Med. Chem. 1996; 4:1135–1147. [PubMed: 8831986]
17. Frey PA, Hegeman AD, Ruzika FJ. The radical SAM superfamily. Critical Rev. Biochem. Mol. Biol. 2008; 43:63–88. [PubMed: 18307109]
18. Chih HW, Marsh ENG. Pre-steady-state kinetic investigation of intermediates in the reaction catalyzed by adenosylcobalamin-dependent glutamate mutase. Biochemistry. 1999; 38:13684–13691. [PubMed: 10521275]
19. Chih H-W, March NG. Mechanism of glutamate mutase: Identification and kinetic competence of acrylate and glycyl radical as intermediates in the rearrangment of glutamate to methylaspartate. J. Am. Chem. Soc. 2000; 122:10732–10733.
20. Banerjee R. Radical carbon skeleton rearrangements: catalysis by coenzyme B12-dependent mutases. Chem. Rev. 2003; 103:2083–2094. [PubMed: 12797824]
21. Sofia HJ, Chen G, Hetzler BG, Reyes-Spindola JF, Miller NE. Radical SAM, a novel protein superfamily linking unresolved steps in familiar biosynthetic pathways with radical mechanisms: functional characterization using new analysis and information visualization methods. Nucleic Acids Res. 2001; 29:1097–1106. [PubMed: 11222759]

22. Nicolet Y, Drennan CL. AdoMet radical proteins--from structure to evolution--alignment of divergent protein sequences reveals strong secondary structure element conservation. Nucleic Acids Res. 2004; 32:4015–4025. [PubMed: 15289575]
23. Wang SC, Frey PA. S-adenosylmethionine as an oxidant: the radical SAM superfamily. Trends Biochem. Sci. 2007; 32:101–110. [PubMed: 17291766]
24. Marsh ENG, Patterson DP, Li L. Adenosyl radical: reagent and catalyst in enzyme reactions. Chem Bio Chem. 2010; 11:604–621.
25. Bonifacic M, Stefanic I, Hug GI, Armstrong DA, Asmus K-D. Glycine decarboxylation: the free radical mechanism. J. Am. Chem. Soc. 1998; 120:9930–9940.
26. Kriek M, Martins F, Challand MR, Croft A, Roach PL. Thiamine biosynthesis in *Escherichia coli*: identification of the intermediate and by-product derived from tyrosine. Angew. Chem. Ind. Ed. 2007; 46:9223–9226.
27. Driesener RC, et al. [FeFe]-hydrogenase cyanide ligands derived from S-adenosylmethionine-dependent cleavage of tyrosine. Angew. Chem. Int. Ed. 2010; 49:1687–1690.
28. Chatterjee A, et al. Reconstitution of ThiC in thiamine pyrimidine biosynthesis expands the radical SAM superfamily. Nat. Chem. Biol. 2008; 4:758–765. [PubMed: 18953358]
29. Acker MG, Bowers AA, Walsh CT. Generation of thiocillin variants by prepeptide gene replacement and in vivo processing by *Bacillus cereus*. J. Am. Chem. Soc. 2009; 131:17563–17565. [PubMed: 19911780]
30. Bowers AA, Acker MG, Koglin A, Walsh CT. Thiazolyl peptide antibiotic biosynthesis: a cascade of posttranslational modifications on ribosomal nascent proteins. J. Am. Chem. Soc. 2010; 132:7519–7527. [PubMed: 20455532]
31. Kriek M, et al. Thiazole synthase from *Escherichia coli* - an investigation of the substrates and purified proteins required for activity *in vitro*. J. Biol. Chem. 2007; 282:17413–17423. [PubMed: 17403671]

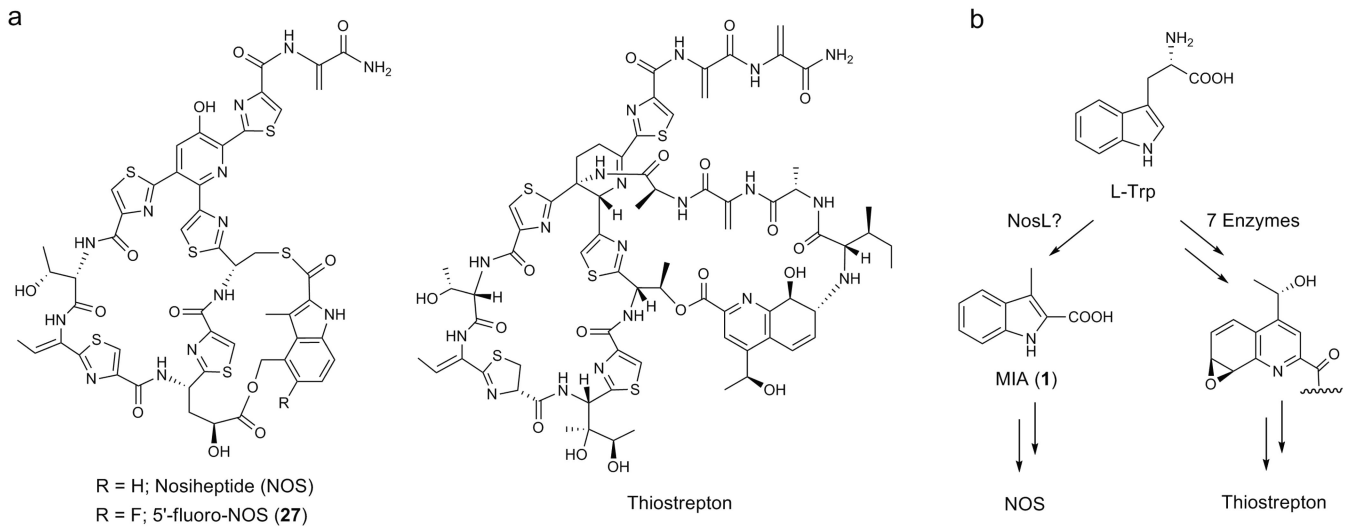

Fig. 1.

Structures of polycyclic thiopeptides and their side ring formations. (a) NOS and 5'-fluoro-NOS, and thiostrepton. (b) Processing of L-Trp to afford the indolic acid moiety of NOS and the quinalic acid moiety of thiostrepton, respectively, via completely different routes.

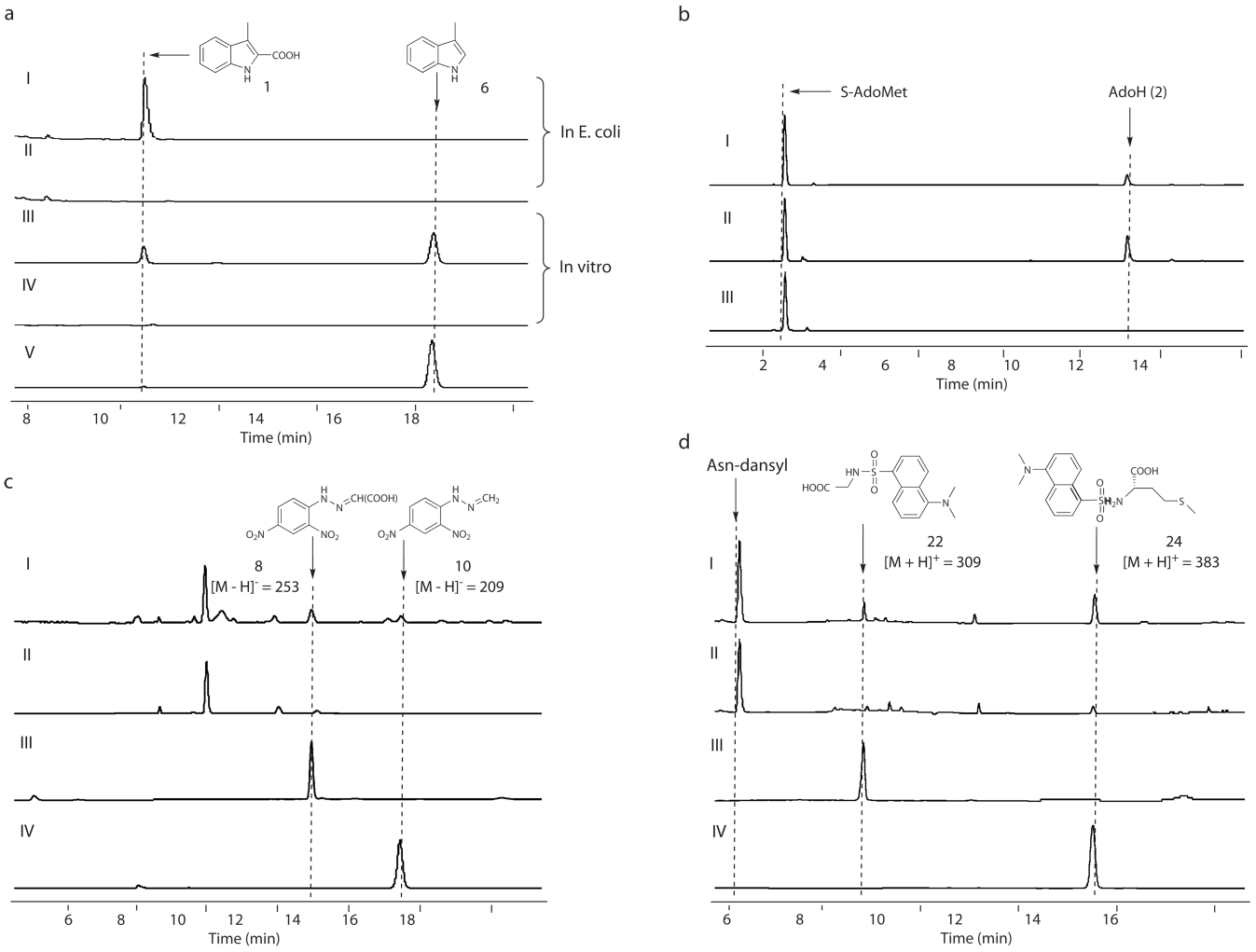

Fig. 2.

Characterization of NosL-catalyzed reaction. All the examinations were performed at least in duplicate (for each having at least two parallel samples). (a) Validation of NosL as a MIA synthase. *In vivo* **1** production in the *E. coli* strains, including SL4101 harboring *nosL* (I) and SL4100 carrying the vector alone (II); and *in vitro* conversion of L-Trp to **1** and the shunt product **6** in the presence (III) and in the absence of *S*-AdoMet (IV), with the authentic **6** as a standard (V). (b) Consumption of *S*-AdoMet given the absence (I) and the presence of L-Trp (II), in contrast to that by omitting NosL from the reaction mixture (III). (c) Identification of the products with DNP derivatization by adding (I) and by omitting the substrate L-Trp (II), when authentic **7** (III) and **9** (IV) were subjected to DNP derivatization to generate the control derivatives. (d) Identification of the putative amino acid products with dansyl chloride derivatization, by using Asn as an internal standard for quantitative analysis. Production in the presence (I) and in the absence of L-Trp (II) while authentic **21** (III) and **23** (IV) were subjected to dansyl derivatization to generate the control derivatives for qualitative analysis.

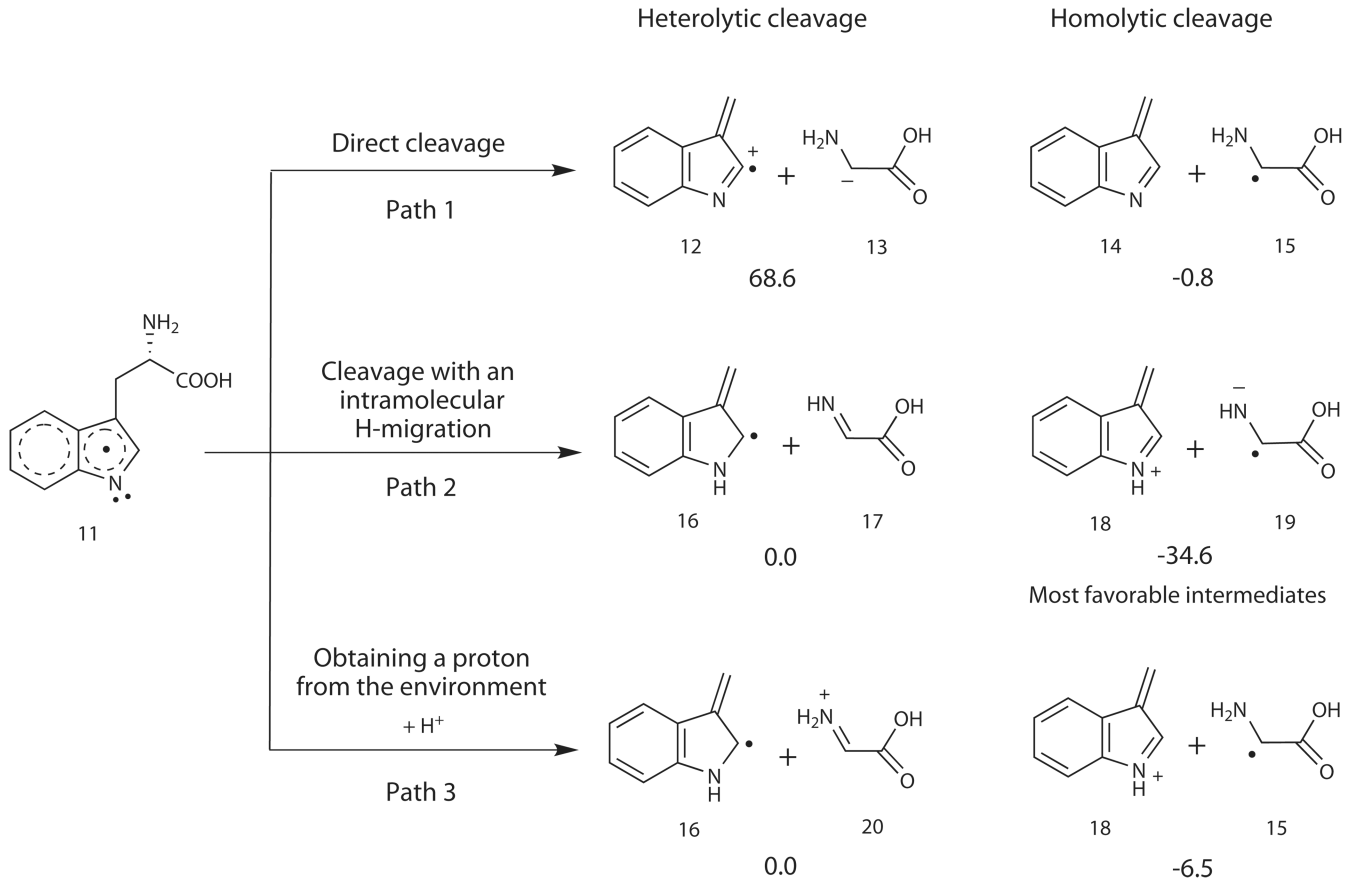

Fig. 3.

Different patterns for cleaving the Cα-Cβ bond of L-Trp neutral radical **11**. The DFT calculation-based, relative free energies (including solvent effect ΔG_{sol}) are in kcal/mol. In **Path 1** and **Path 2** the energy of **16 + 17** is used as the reference zero energy, whereas in **Path 3** the energy of **16 + 20** is used as the reference.

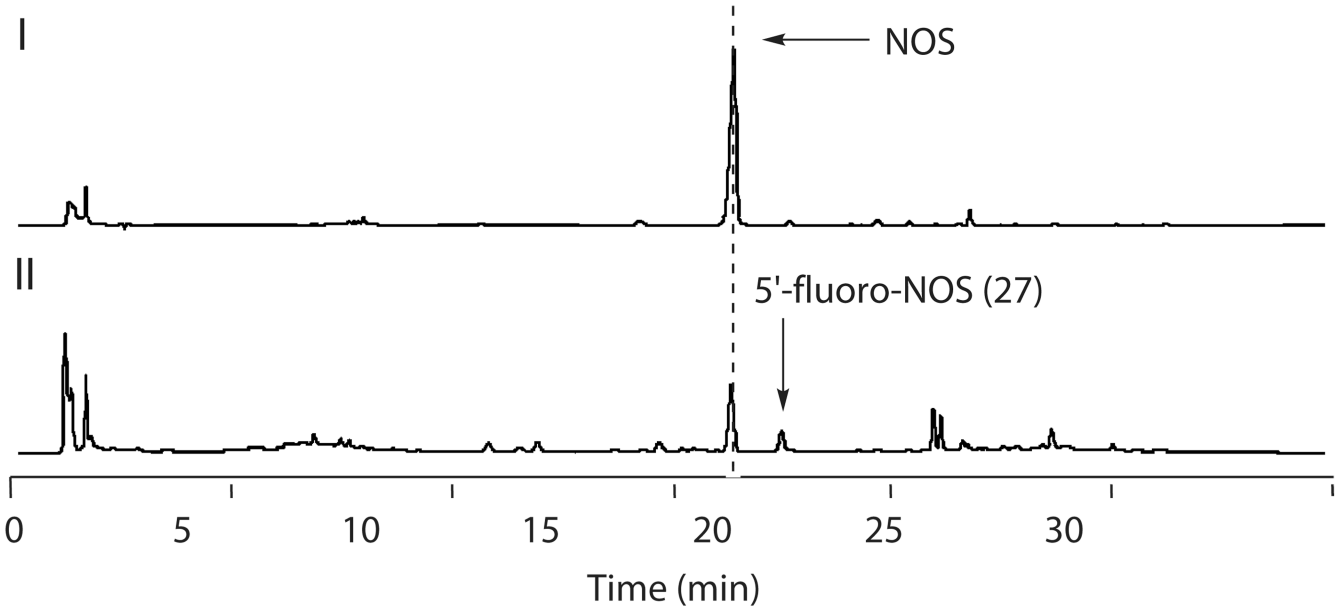

Fig. 4.

Production of NOS and fluorinated thiopeptide by *S. actuosus* without the supplementation (I) and with the supplementation of 5-fluoro-DL-Trp (II). All the examinations were performed in duplicate (for each having two parallel samples).

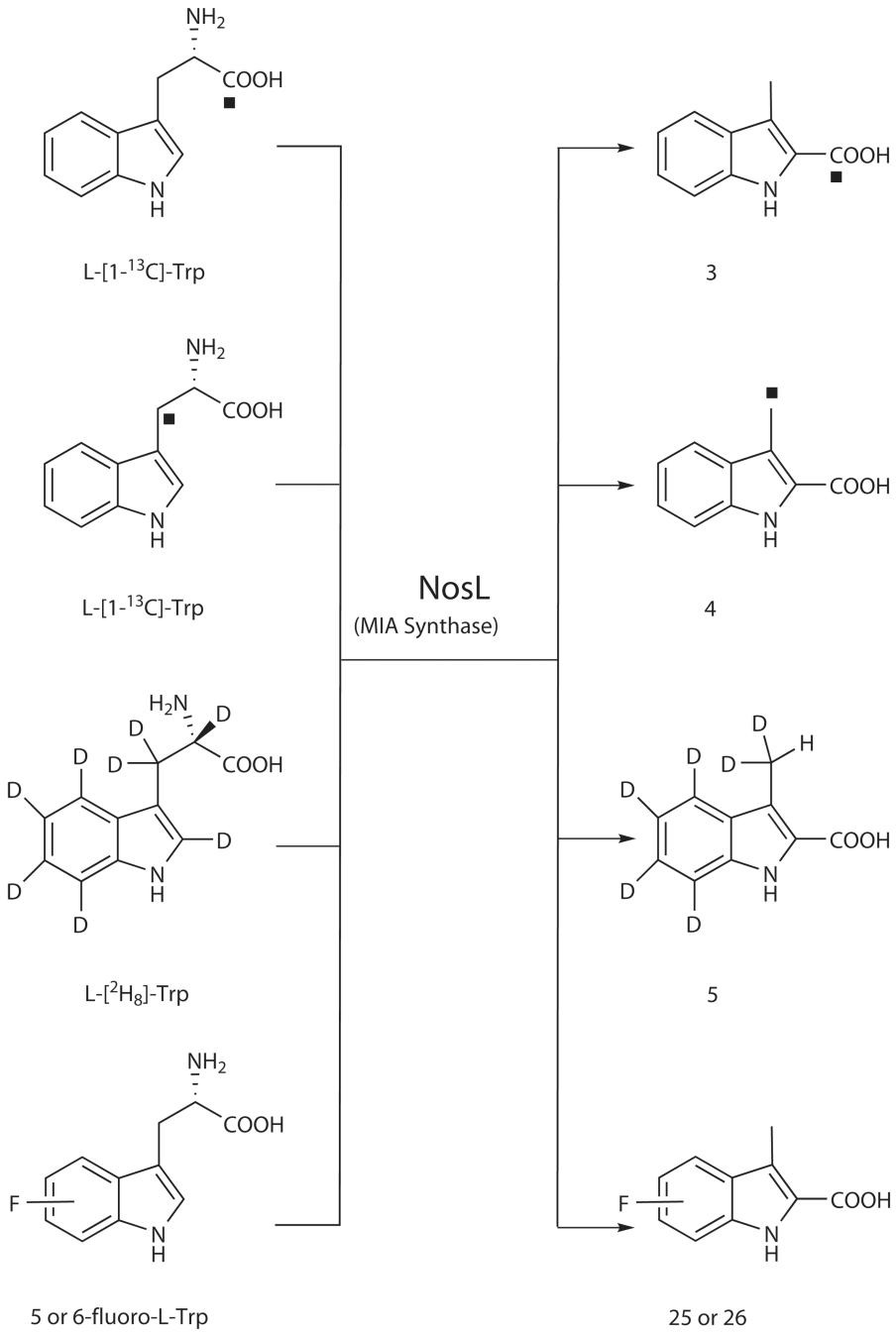

Scheme 1.

NosL-catalyzed carbon chain reconstitution of L-Trp shown by labeling patterns and generation of fluorinated MIA analogues. The solid rectangle shows the ^{13}C-labeled carbon atom. D, deuterium. F, fluorine.

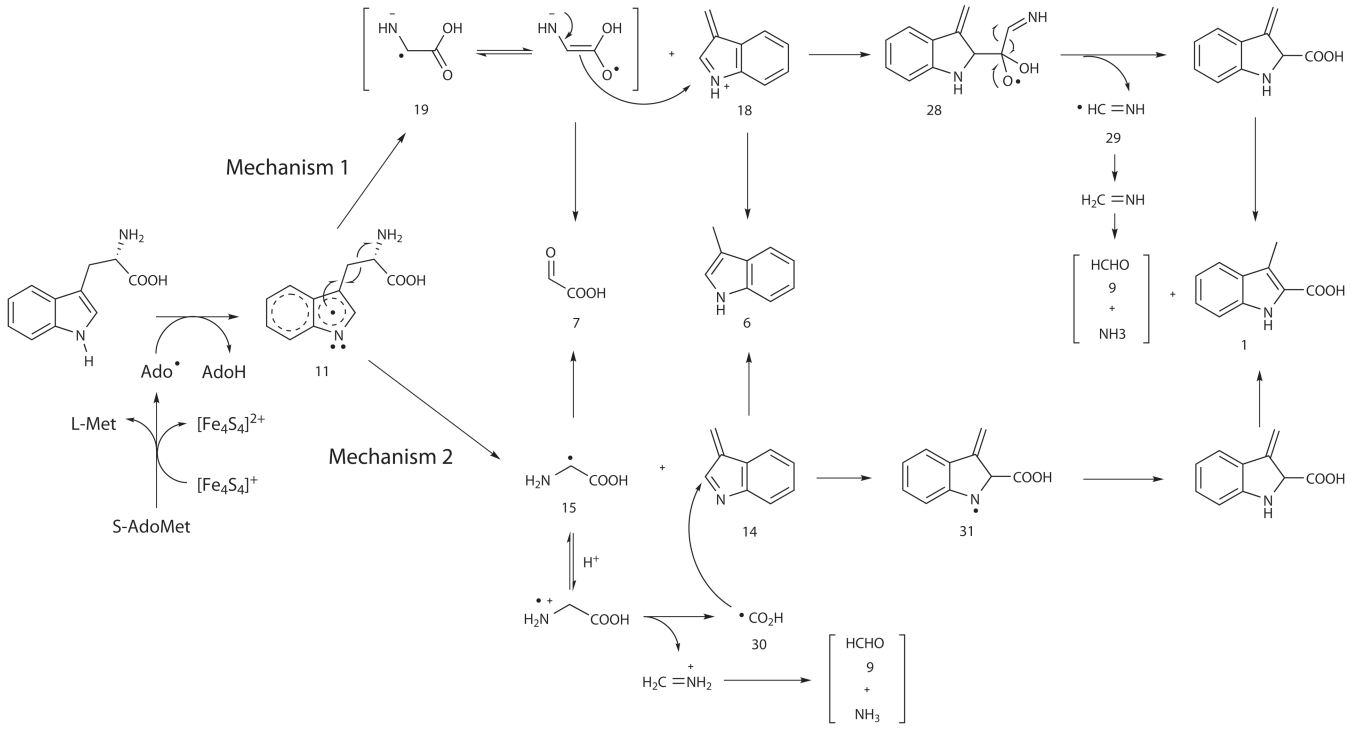

Scheme 2.

Mechanistic hypothesis for NosL-catalyzed conversion. For **Mechanism 1**, the recombination may take place between cationic **18** and radical **19** followed by elimination of the Cα-N unit from the resulting radical **28**; and for **Mechanism 2**, the first separated radical **15** could undergo the second fragmentation to generate carboxyl radical **30** before the addition onto **14**.